Colloid Polym Sci (2006) 284: 1073–1084
DOI 10.1007/s00396-006-1483-x

ORIGINAL CONTRIBUTION

Mallika Das
Eugenia Kumacheva

From polyelectrolyte to polyampholyte microgels: comparison of swelling properties

Received: 13 December 2005
Accepted: 1 March 2006
Published online: 20 May 2006

M. Das · E. Kumacheva (✉)
Department of Chemistry,
University of Toronto,
80 Saint George Street,
University of Toronto,
Toronto, ON M5S 3H6, Canada
e-mail: ekumache@chem.utoronto.ca

Abstract We report the results of comparative studies of the swelling behavior of polyelectrolyte (PE) and polyampholyte (PA) microgels in response to pH, ionic strength, temperature, and solvent composition. Polyelectrolyte microgels used were cross-linked binary copolymers of poly(*N*-isopropylacrylamide) (polyNIPAm) and acrylic acid (AA) or vinyl imidazole (VI). The PA microgels with an excess of either cationic or anionic groups swelled at low *or* high pH values, respectively, analogous to PE microgels. The PA microgels with similar amounts of AA and VI groups exhibited marked swelling at *both* high and low pH values. All PA microgels shrank in the intermediate range of pH due to electrostatic attraction between charged AA and VI moieties. In moderately concentrated salt solutions, PA microgels underwent swelling showing antipolyelectrolyte behavior. The extent of swelling of PA microgels increased with rise in AA content. The temperature-dependent contraction of both PE and PA microgels occurred at higher temperatures when AA and VI groups were charged and hydrophilic. Ion pairing between the AA and VI groups increased the extent of the temperature-induced deswelling in PA microgels. The solvent-dependent swelling of PE and PA microgels in ethanol–water mixtures was governed by competing electrostatic and cosolvency effects.

Keywords Polyampholyte microgels · Zwitterionic · Electrostatic interactions · Swelling behavior

Introduction

Microgels are particles with dimensions in the range 100 nm to 1 μm, which consist of cross-linked polymer networks swollen in a solvent [1]. In the past several decades, microgels have attracted much attention in theoretical studies of soft matter [2] and in applied fields, e.g., materials science [3, 4]. In particular, they have rapidly gained importance due to their potential applications in drug delivery [5–7], ion exchange [8], in sensing [9], in the fabrication of photonic crystals [10, 11], and in template-based synthesis of inorganic nanoparticles [12, 13].

To date, the most intensely studied microgels are based on the neutral, thermo-responsive polymer, poly(*N*-isopropylacrylamide) (polyNIPAm) or related copolymers [1, 14]. Below the lower critical solution temperature (LCST), polyNIPAm is swollen due to hydrogen bonding between the water molecules and amide residues on the polymer backbone; whereas, above the LCST, the hydrogen bonds are disrupted, and the increased intra- and interchain polymer interactions contract the polymer network [15, 16]. Incorporation of ionic groups into the neutral polyNIPAm network gives rise to polyelectrolyte (PE) microgels [17]. Recent studies on polyelectrolyte microgels were motivated by their multi-responsive nature as exhibited by their ability to respond to a number of stimuli including change in temperature [18–20], pH [21], ionic strength of the medium [22], and electric fields [23].

Polyelectrolyte microgels that contain both positive and negative charges along the polymer chain are called

polyampholyte (PA) microgels [24]. The properties of polyampholyte microgels are very different from those of polyelectrolyte microgels due to the presence of oppositely charged groups in the polymer network. From a scientific perspective, PA microgels are fascinating systems, due to the multiple interactions acting in parallel with or competing against each other within the microgel interior. In the last decade, significant efforts have focused on the swelling behavior of macroscopic PA gels. For these systems, the response times are on the order of several hours: the characteristic response time, τ, of a gel is given by $\tau = l^2/\pi^2 D$ where l is the characteristic linear size of the gel and D is the diffusion coefficient of the network [25, 26]. By contrast, microgels offer significantly faster response times, often on the order of seconds or even fractions of seconds [27, 28].

Ogawa et al. reported the results of systemic studies of the response of PA microgels to variations in temperature, pH, and salt concentration in the dispersion medium [29]. The authors did not report any appreciable change in size for PA microgels characteristic of polyampholyte behavior. They did, however, observe enhanced colloid stability for the microgels with similar numbers of acidic and basic groups in salt solutions, in comparison with the stability in pure water. Conversely, PA microgels with an excess of cationic or anionic groups exhibited greater stability in pure water, but aggregated at higher salt concentrations. The authors attributed these results to intra- and interparticle interactions were not solely dependent on electrostatic interactions but originated from hydrogen bonding and hydrophobic association, as well.

Nayak and Lyon showed that PA microgels synthesized by copolymerization of NIPAm, acrylic acid (AA), and *N*-(3-aminopropyl) methacrylamide exhibited zwitterionic behavior in a particular pH range [30]. Temperature-dependent volume transitions of microgels with similar numbers of oppositely charged groups were sharper in the zwitterionic range of pH than at a non-zwitterionic pH, due to the closer proximity of oppositely charged groups that formed attractive ion pairs and facilitated the expulsion of water from the microgel interior.

While the aforementioned papers provided valuable insight into the behavior of PA microgels, there has not yet been a comprehensive study of the similarities and differences between the swelling behavior of polyelectrolyte and polyampholyte microgels, though properties of macroscopic PA gels have been extensively studied by Tanaka [22, 24–26, 31, 32]. Furthermore, the effect of the compositions of the dispersion medium on the swelling behavior of PA microgels has not previously been considered. The effect of solvent is important in two respects: (a) osmotic interactions between the monomer residues compete with, or enhance their interactions with the solvent (b) the strength of the electrostatic forces acting in the microgels depends on the dielectric constant of the solvent and the extent of dissociation of ionic groups.

The present paper endeavoured to compare polyelectrolyte and polyampholyte microgels with the aim of gaining a deeper understanding of the differences and similarities in their swelling behavior in response to the variations in pH, temperature, ionic strength, and solvent composition. Anionic and cationic polyelectrolyte microgels were obtained by copolymerization of *N*-isopropylacrylamide and AA or copolymerization of *N*-isopropylacrylamide and vinyl imidazole (VI). Polyampholyte microgels with different compositions were obtained by copolymerization of *N*-isopropylacrylamide with various amounts of acrylic acid and vinyl imidazole.

Background

Volume transitions in polymer gels result from competing attractive and repulsive interactions, namely, polymer rubber elasticity and osmotic swelling [33]. Other governing factors include H-bonding, hydrophobic forces, van der Waals forces, coulombic interactions, osmotic pressure due to the counter ions, and specific forces (e.g., biotin–strepavidin interactions) [32]. All forces acting in PE microgels are present in PA microgels; however, coulombic interactions in PA and PE microgels are fundamentally different. A schematic illustration of the electrostatically driven volume transitions in PE and PA microgels is depicted in Fig. 1. When a change in pH leads to ionization of the acidic or basic groups (Fig. 1a and b, respectively) the resulting electrostatic repulsion between the like charges causes the network to swell, leading to an increase in particle size. Fig. 1c shows a schematic of the swelling–deswelling transitions of PA microgels. At low pH, swelling is enhanced by the repulsion between protonated basic residues in the polymer network, while at high pH, swelling is attributed to repulsion between negatively charged species. In the interim region of pH (the "zwitterionic region") a relatively large fraction of both positively and negatively charged groups is present in the PA microgels. Ion pairing between the oppositely charged groups dominates over repulsion between unpaired like charges, leading to microgel shrinkage. Thus, the PA microgels attain their smallest size at the isoelectric point (p*I*) in the zwitterionic region.

Experimental

Materials *N*-isopropylacrylamide, acrylic acid, vinyl imidazole, *N*-*N*′-methylene-bis-acrylamide) (BIS), potassium persulfate (KPS), and sodium dodecyl sulfate (SDS) were purchased from Aldrich Canada and used as received. Deionized water with a resistance of 18.2 MΩ (Millipore Milli-Q) was used.

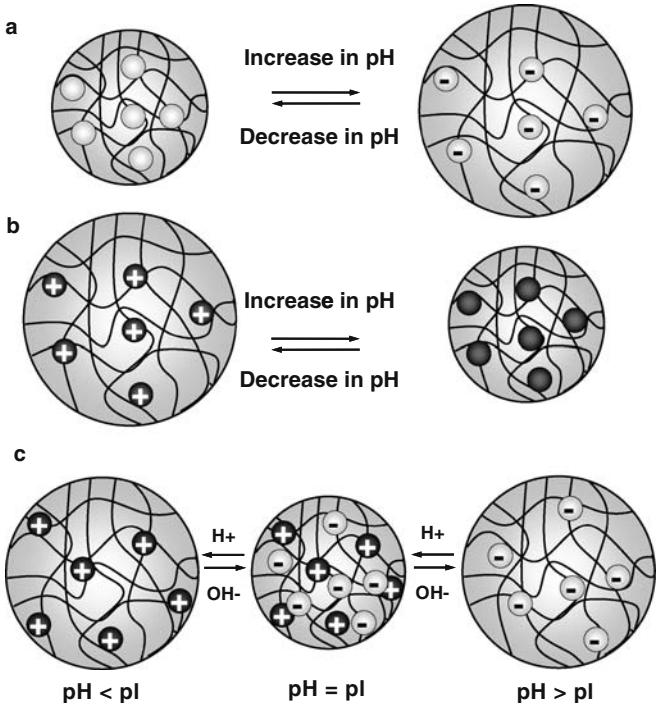

Fig. 1 Schematic illustration of the swelling mechanism of polyelectrolyte and polyampholyte microgels. **a** Anionic *PE* microgels. Ionization of the anionic groups at high pH and resultant electrostatic repulsion between them causes microgel swelling. **b** Cationic PE microgels. At low pH, electrostatic repulsion between ionized cationic groups causes microgel swelling. **c** Polyampholyte (*PA*) microgels. The PA microgels are swollen at low and high pH values, due to repulsion between charged cationic and anionic groups, respectively. In the interim pH region, PA microgels have zwitterionic properties and contract due to electrostatic attraction between the oppositely charged groups. For simplicity, counterions are omitted

Synthesis of microgels The microgels were prepared via free radical precipitation polymerization. The monomers, surfactant, and cross-linker were dissolved in 85 ml of deionized water, degassed for 30 min and then heated to 65 °C in the nitrogen atmosphere. Potassium persulfate was dissolved in 15 ml of deionized water and injected into the reaction mixture. The reaction was carried out for 5 h at 65 °C under a steady stream of nitrogen in a three-necked round bottom flask equipped with a condenser and a stirrer. Originally, we followed the procedures of Vincent [1] and Pelton [17] for the purification of monomers before microgel synthesis. We found no notable difference in the microgel composition or size, based on light scattering data, titrations, and SEM imaging. Thereafter, we used monomers "as received." The concentration of NIPAm in the reaction mixture was kept constant at 82.3± 1.3 mol% while the ratios of AA/VI were changed as shown in Table 1. After polymerization was complete, the microgel dispersion was purified by dialysis against deionized water for 14 days (daily changes of water, Spectra/Por Membrane, MWCO: 12-14,000). Dialysis, even over extended periods, was not always sufficient to remove all linear polymers or sol from microgel dispersions. However, a combination of dialysis and repeated centrifugation, decantation, and redispersion techniques at tuned pH can quite effectively remove linear polymers, from a dispersion of microgels ca 200 nm in diameter.

Particle characterization Particle dimensions were determined by photon correlation spectroscopy (PCS, Protein Solutions). The hydrodynamic radii of the microgels were calculated based on the measured diffusion coefficients by using the Stokes–Einstein equation. Measurements of electrokinetic potential of the microgels were conducted using the Zetasizer 3000HSA (Malvern instruments, U.K.). Each sample was allowed to equilibrate for 10 min at the desired temperature before data collection. Simultaneous potentiometric and conductometric titrations with NaOH or HCl were performed to determine the approximate amounts of AA and VI residues in the PE microgels, respectively. At the beginning of the titration, the PE microgels were acidified or alkalized to ensure that AA or VI residues were in their uncharged state. Three regions were observed in the titration curves of PE microgels, plotted as the variation in conductivity of the system vs volume of titrant. In the first

Table 1 Compositions and characteristics of polyelectrolyte and polyampholyte microgels

	Monomer compositions in reaction mixture[a] (mol%)			Functional groups/particle[b]			Rh (nm)[c]	p*I*
	[NIPAM]	[AA]	[VI]	$N_{acidic}\times10^4$	$N_{basic}\times10^4$	N_{acidic}/N_{basic}		
PE-NAA	83.2	21.9	0	33.6			75	
PE-NVI	82.4	0	17.4		37.9		143	
PA-0.46	83.6	7.3	5.6	3.9	8.5	0.46	79	5.81
PA-0.90	83.3	8.7	4.5	34.3	38.6	0.90	74	5.61
PA-1.25	81.1	11.3	4.3	34.3	38.6	0.90	74	5.61
PA-1.65	82.7	11.5	2.2	8.8	5.3	1.65	57	4.75

[a]The concentrations of SDS and BIS in the reaction mixture were 0.05 and 3.5–4 mol%, respectively
[b]Data obtained from conductometric titration
[c]Hydrodynamic radius, R_h, was measured at room temperature in 0.01 M KCl solution. For PE and PA microgels, R_h was measured at pH=pk_a and pH=p*I*, respectively

region, the conductivity of the dispersion decreased with neutralization of excessive H^+ or OH^- ions that were present due to pre-acidification or pre-alkalization. In the second region, ionization of acidic or basic groups in the polymer caused an increase in conductivity, and hence, the slope of curve conductivity vs the volume of the titrant. In the third region, the slope was equal to the theoretical conductivity of the titrant (NaOH or HCl). The intersection of the extrapolated lines drawn as tangents to the titration curve in the first and the third regions yielded the equivalence point and provided the number of consumed moles of H^+ or OH^- as

$$\text{Moles of } H^+ = [(N_{HCl} \times V_{HCl}) - (N_{NaOH} \times V_{NaOH}(\text{consumed}))]$$
$$\text{Moles of } OH^- = [(N_{NaOH} \times V_{NaOH}) - (N_{HCl} \times V_{HCl}(\text{consumed}))]$$

where V is the volume of NaOH or HCl given in ml.

The conductometric titration curves for PA microgels contained four regions. Acidification of the PA microgels to pH=3 before titration ensured that the AA residues were uncharged and that VI groups were protonated; thus, interaction between the opposing ionized groups was minimized. As the values of pk_a for AA and VI are 4.26 and 6.94, respectively, AA groups were titrated, first. When titrating against NaOH, the first two regions of the titration curves of PA microgels were similar to that of PE microgels; in the third region, conductivity slightly decreased with neutralization of protonated VI residues, and in the fourth region, conductivity increased due to the presence of free OH^- ions. The intercepts of the slopes to the titration curves in the second and third regions and in the third and fourth regions yielded the end points with respect to COOH and $=NH^+$ groups, respectively. Although, some interaction between the charged VI and AA groups in the zwitterionic pH regime may have occurred, the end points obtained from both conductometric and potentiometric titrations were verified by comparison with the value of pH at the isoelectric point as determined from electrokinetic potential measurements of the microgels. We found reasonable agreements among all three values.

The number of $-COO^-$ and/or $\equiv NH^+$ groups in the microgels was calculated as [34]

$$N_{COO^-} = [(\text{moles of } H^+)N_{Av}]/\text{number of particles per unit volume} \quad \text{or}$$
$$N_{NH^+} = [(\text{moles of } OH^-)N_{Av}]/\text{number of particles per unit volume} \qquad (1)$$

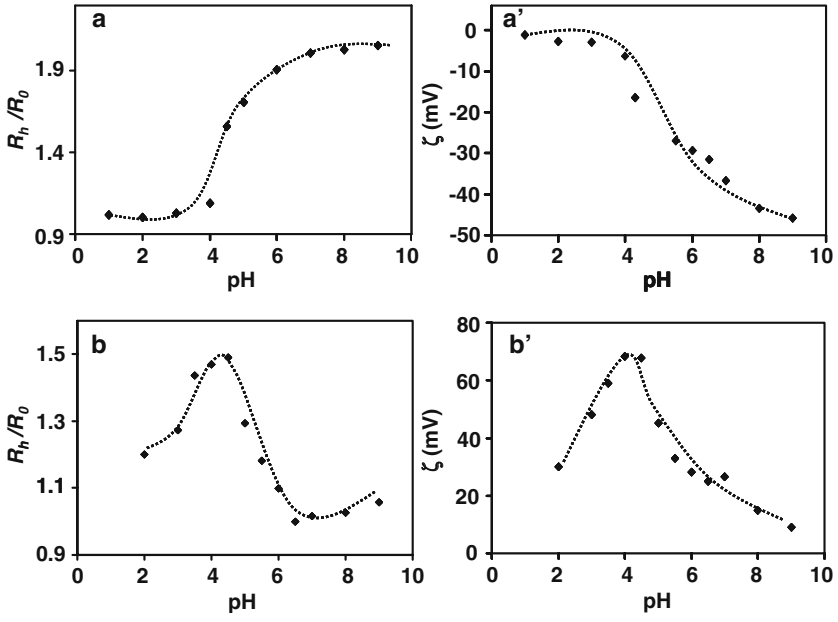

Fig. 2 Variation in R_h/R_0 (**a**, **b**) and electrokinetic potential (ζ-potential) (**a'**, **b'**) of *PE* microgels as a function of pH: **a**, **a'** poly(NIPAm-AA), R_0=75 nm; **b**, **b'** poly(NIPAm-VI), R_0=143 nm. The *dashed curves* are given for eye guidance

where N_{Av} is the Avogadro number, $N_{Av}=6.023\times10^{23}$ molecules mol^{-1}.

The number of particles per unit volume was estimated as V/v_i, where V is the total volume of particles per unit volume of dispersion (ml) and v_i is the mean volume of a particle. The values V and v_i were found as

$$V = \frac{W(g)}{\rho\left(g\,ml^{-1}\right)} \tag{2}$$

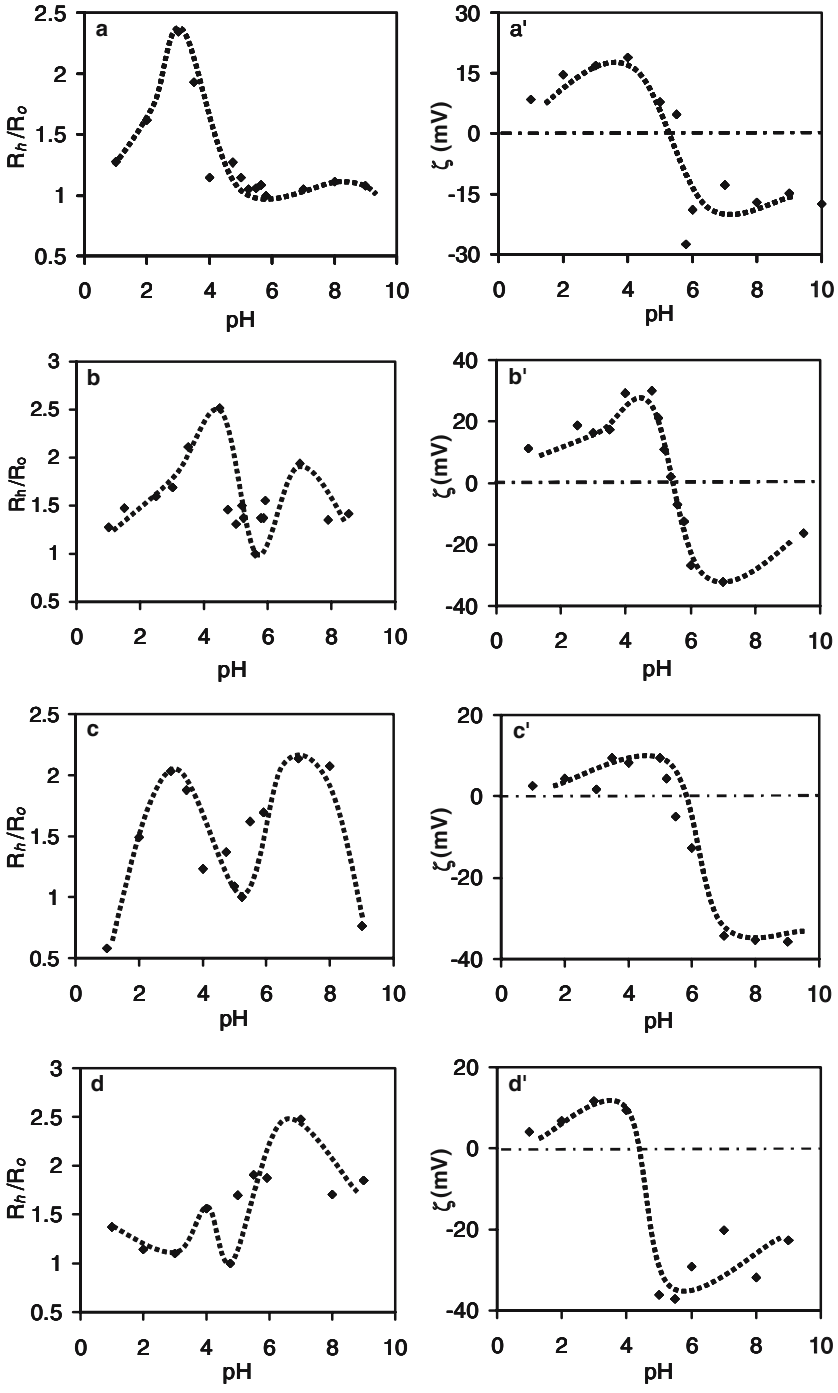

Fig. 3 Effect of pH on the variation in R_h/R_0 (**a**–**d**) and ζ-potential (**a**'–**d**') for polyampholyte microgels in 0.01-M KCl solution at 25 °C: **a**, **a**' PA-0.46, R_0=79 nm ; **b**, **b**' PA-0.9, R_0=73.8 nm; **c**, **c**' PA-1.25, R_0=59.6 nm; **d**, **d**' PA-1.65 R_0=57.2 nm. *Dashed lines* are drawn as eye guidelines. The *horizontal dashed line* demarks ζ-potential=0

where W is the mass of "wet" microgel in a dialyzed dispersion, isolated by filtering microgels (pore size, 0.22 μm) at pI and ρ is the density. As the microgel particles were highly swollen in water, we assumed ρ=1 g ml^{-1}.

The value of v_i, was determined by

$$\nu_i = 4/3\left(\pi R_h^3\right) \quad (3)$$

The data thus obtained from titrations and measurements of electrokinetic potential is presented in Table 1, along with the molar ratio of acidic/basic groups, the isoelectric point of PA microgels, and microgel size.

Results

After synthesis, microgels with different fractions of AA and VI had different dimensions. To compare the effect of the variation of pH, ionic strength, temperature, and ethanol concentration in the dispersion medium on microgel swelling, we presented the change in particle size as the variation in *normalized* hydrodynamic radius of microgels (R_h/R_0), where R_h is the average hydrodynamic radius of particles at a particular pH, salt concentration, temperature, or solvent composition, and R_0 is the smallest hydrodynamic radius measured in a particular series of experiments.

Effect of pH Figure 2 shows the variation in the normalized microgel size (left), R_h/R_0, and electrokinetic potential (right) of PE microgels. In Fig. 2a, the value of R_h/R_0 of the anionic poly(NIPAm-AA) microgels remained almost constant at 1.0<pH<4.0 while in the range 4.0<pH<5.5, a steep swelling transition occurred. The increase in size was attributed to electrostatic repulsion between –COO$^-$ groups (pk_a of AA=4.25) [35]. The particles continued to swell at pH>5.5, ultimately reaching a 100% increase in size compared to that at low pH. The variation in electrokinetic potential (Fig. 2a') correlated with the change in microgel size in the same pH range. At pH<4.0, the value of ζ-potential was close to zero, implying that most of the –COOH groups of AA were not dissociated, whereas, in the range 4.0<pH<9.0, the value of ζ-potential reduced to reach the value of ca −46 mV.

Figure 2b and b' shows the variation in size and electrokinetic potential respectively, of cationic poly (NIPAm-VI) microgels as a function of pH. The microgels rapidly swelled with increasing acidity in the range 4.0<pH<6.5 (Fig. 2b). The swelling was ascribed to repulsion between the protonated imidazole groups at pH<7.0 (pk_a of VI is 6.99 [36, 37]). The dependence of ζ-potential vs pH (Fig. 2b') followed the trend in the variation of particle size with the maximum value of ζ-potential at pH≈4.0, indicating the dominance of coulombic forces in variation of microgel size. Decrease in microgel size in the range 2.0<pH<4.0 was attributed to the increased ionic strength of the medium.

Figure 3 shows the variation in R_h/R_0 and ζ-potential as a function of pH for PA microgels with different fractions of cationic and anionic residues. Figure 3a–d (left column) shows that all PA microgels displayed a similar trend: strong shrinking at 4.0<pH<7.0 (the largest contraction occurring at the isoelectric point), and two swelling regions on either side of the isoelectric point (ζ-potential=0). As the values of pk_a of AA and VI are 4.25 [26] and 6.99[1], respectively, in the range corresponding to microgel shrinkage, the particles carried both positive and negative charges, that is, showed zwitterionic behavior (corroborated by ζ potential measurements, Fig. 3a'–d'). Increase in the molar ratio of anionic-to-cationic residues had two consequences: the shift of pI towards lower values of pH and the change in the shape of the curve R_h/R_0. The former effect arose because the number of COO$^-$ groups outnumbered the number of NH≡$^+$ groups: thus, increased acidity was required to protonate the excess COO$^-$ groups (that were not neutralized by NH≡$^+$ moieties) to reach the isoelectric point. The latter feature revealed itself in the different extents of swelling of the PA microgels with different compositions. For example, at pH=4.0, the higher content of VI in PA-0.46 compared to PA-1.65 was reflected by the values of R_h/R_0 of ca 2.5 and 1.5, respectively (left 'humps' in Fig. 3a and d, respectively). Similarly, at pH=7.0, the higher AA content in PA-1.65 vs PA-0.46 resulted in R_h/R_0 values of ca 2.6 and 1.0, respectively (right "humps" in Fig. 3d and a, respectively). Thus, the swelling profile of PA microgels with a large fraction of VI resembled that of cationic PE microgels (Fig. 2b). Likewise, the swelling curve of microgels with a large fraction of AA (Fig. 3d) resembled the anionic PE microgels (Fig. 1a). By contrast, PA microgels with more symmetric compositions (PA-0.9 and PA-1.25) showed relatively similar extents of swelling on either side of the pI: two distinct swelling regions with a maximum ratio R_h/R_0 of ca 2.5 (Fig. 3b,c).

Effect of ionic strength We examined the effect of ionic strength on the swelling properties of PE and PA microgels by diluting dispersions with KCl solution of different concentrations and measuring the variation in particle size. Figure 4a shows the variation in normalized size of poly (NIPAm-AA) microgels (pH=7.0) and poly(NIPAm-VI) microgels (pH=4.0) as a function of electrolyte concentration. In both dispersions, increase in the concentration of KCl from 10^{-5} M to 2.0 M resulted in contraction of the microgels. The total shrinkage observed for poly(NIPAm-

[1] The pk_a value in a polymer is subject to the fluctuations in local charge density, ionic strength and pH of the medium, microstructure (blockiness/randomness), crosslinker concentration and polymer composition—all of which can cause it to vary significantly. The values of pk_a reported for imidazole in the literature therefore do vary between 5 and 10 [36–41].

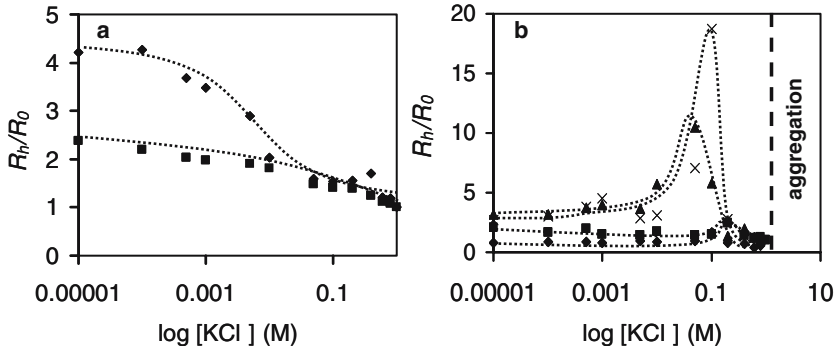

Fig. 4 **a** Variation in normalized hydrodynamic radius (R_h/R_0) as a function of KCl concentration for polyelectrolyte microgels: (♦) poly(NIPAm-AA), pH=7.0, T=25 °C, R_0=22.6 nm; (▪) poly(NIPAm-VI), pH=4.0, T=25 °C, R_0=91 nm. **b** Variation in normalized hydrodynamic radius (R_h/R_0) as a function of KCl concentration for polyampholyte microgels: (♦) PA-0.46, R_0=24.5 nm (▪) PA-0.9), R_0=44.2 nm (▲) PA-1.25, R_0=28.6 nm (×) PA-1.65, R_0=24.5 nm; pH=pI, T=25 °C

AA) and poly(NIPAm-VI) microgels was ca 75 and 50%, respectively. Such polyelectrolyte behavior was typical of polyelectrolytes in salt solutions [41]. No particle aggregation was noticed up to KCl concentration of 1 M.

Volume transitions of PA microgels were studied at their respective pI values. Figure 4b shows the swelling profiles of PA microgels with different compositions as a function of KCl concentration. At salt concentrations below 0.005 M, no significant change in microgel size was observed. A notable swelling peak occurred at higher salt concentrations for all PA microgels indicating their antipolyelectrolyte behavior. We did not observe any discernable correlation between the asymmetric and symmetric compositions of PA microgels and their swelling profiles. Instead, we found that increasing AA content PA microgels led to larger swelling ratios in the range 0.005 M<[KCl]<0.4 M: for example, the values of R_h/R_0 for PA-0.46 and PA-1.65 were 1.7 and 18, respectively. The tremendous increase in microgel size occurred *not* due to particle flocculation: the light scattering data showed relatively narrow size distributions and negligible change in scattering intensity. At higher concentrations of KCl, the microgels aggregated due to suppressed electrostatic interactions between them.

Effect of temperature Figure 5a,b shows the variation in hydrodynamic radius of PE microgels as a function of temperature. For each system, measurements were conducted at two critical values of pH: one that rendered the microgels ionic and more hydrophilic and the other that made them almost neutral and relatively hydrophobic. Note that all VPTTs measured in the current work were determined by monitoring the change in hydrodynamic radii of microgels. Figure 5a shows that the value of R_h/R_0 for poly(NIPAm-AA) microgels in the entire temperature range studied was significantly larger at pH=7.0 than at pH=3.5. The volume phase transition temperature (VPTT) was ca 30 °C at pH=3.5 and 55 °C at pH=7.0. The shift of VPTT at pH=3.5 to a value lower than that of homopolymer polyNIPAm microgels (ca 32 °C) [41] was due to the decreased hydrophilicity of AA [42–44]. At pH=7.0, the shift of VPTT to a higher value than that of homopolymer polyNIPAm microgels (ca 32 °C) [41] was attributed to the increased hydrophilicity of, and the repulsion between, ionized AA segments [26]. Similarly, for poly(NIPAm-VI)

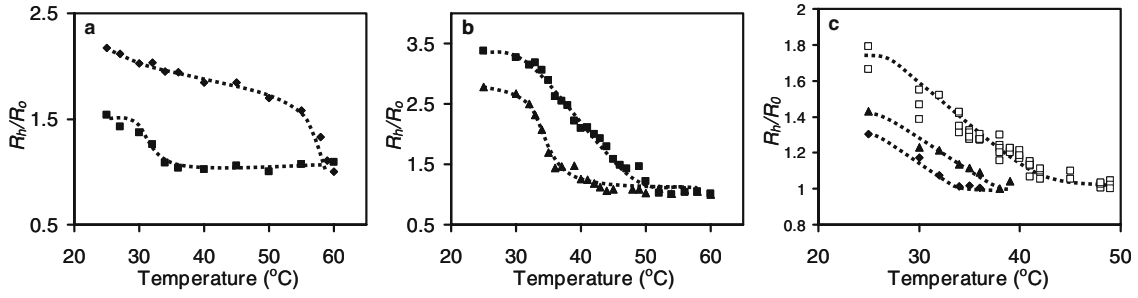

Fig. 5 Variation in microgel size as a function of temperature: **a** poly (NIPAm-AA) microgels, (▪) pH=3.5, R_0=50 nm, (♦) pH=7.0, R_0=69.5 nm; **b** poly(NIPAm-VI) microgels, (▪) pH=4.0, R_0 = 63.9 nm, (♦) pH=7.5, R_0=52.6 nm; **c***PA* microgels with various compositions at corresponding pI values, (♦) PA-0.46, R_0=49.8 nm; (π) PA-1.65, R_0=35.9 nm; (□) PA-1.25, R_0=42.4 nm. R_h is the hydrodynamic radius of microgels at a particular temperature and R_0 is the minimum R_h observed just before aggregation of *PA* microgels. All microgels were studied in 0.1-M KCl solution. *Dashed lines* are given for eye guidance

microgels (Fig. 5b), protonation of the imidazole groups and augmented hydrophilicity of the microgels shifted the VPTT to ca 35 °C at pH=4.0 (vs 31 °C at pH=7.5).

Figure 5c shows the temperature dependence of volumes of PA microgels with different compositions, determined at the corresponding p*I* values. Note that all PA microgels coagulated with increase in temperature, in contrast to PE microgels which showed no coagulation in the temperature range studied. Symmetric PA microgels displayed greater colloidal stability than asymmetric PA microgels: coagulation occurred above 48 °C in the former, compared to above 37 °C in the latter systems. Before the loss of colloid stability, the PA microgels featured gradual deswelling. The strongly asymmetric PA-0.46 and PA-1.65 microgels underwent ca 23 and 30% shrinkage, respectively, when they were heated from 25 to 37 °C. The symmetric PA-1.25 microgels showed stronger reduction in the size of ca 43 at 48 °C.

Effect of solvent Figure 6a–e shows the variation in normalized size of PE and PA microgels at different pH values (corresponding to charged and neutral microgel states) as a function of the volume fraction of ethanol, ϕ, added to the aqueous medium. In Fig. 6a, for poly (NIPAm-AA) microgels, a clear minimum in R/R_0 was observed at ϕ=0.5. The extent of swelling of these microgels in the deprotonated state (pH=7.5) was three times as large as in the protonated state (pH=4.0). By contrast, poly(NIPAm-VI) microgels (Fig. 6b), remained shrunken in both protonated and deprotonated states at $\phi \tilde{\leq} 0.4$ while in the region $0.4<\phi<0.5$, the value of R_h/R_0 abruptly increased. The increase was steeper at pH=4.0, corresponding to the ionized state of the microgels. At larger values of ϕ, the particles shrank at pH=4.0 and continued to increase in size at pH=7.5. Figure 6c–e shows the change in R_h/R_0 for the PA microgels with strongly asymmetric and symmetric compositions as a function of $\tilde{\phi}$. A marked swelling maximum was observed at $\phi \approx 0.5$ in all PA microgels, irrespective of pH range.

Consider first PA-0.46, the microgel with asymmetric composition (Fig. 6c). As in this system VI was present in the largest and AA in the smallest amount, its swelling behavior was anticipated to resemble that of poly(NIPAm-VI) microgels. Contrary to expectations, at pH=4.0 (when

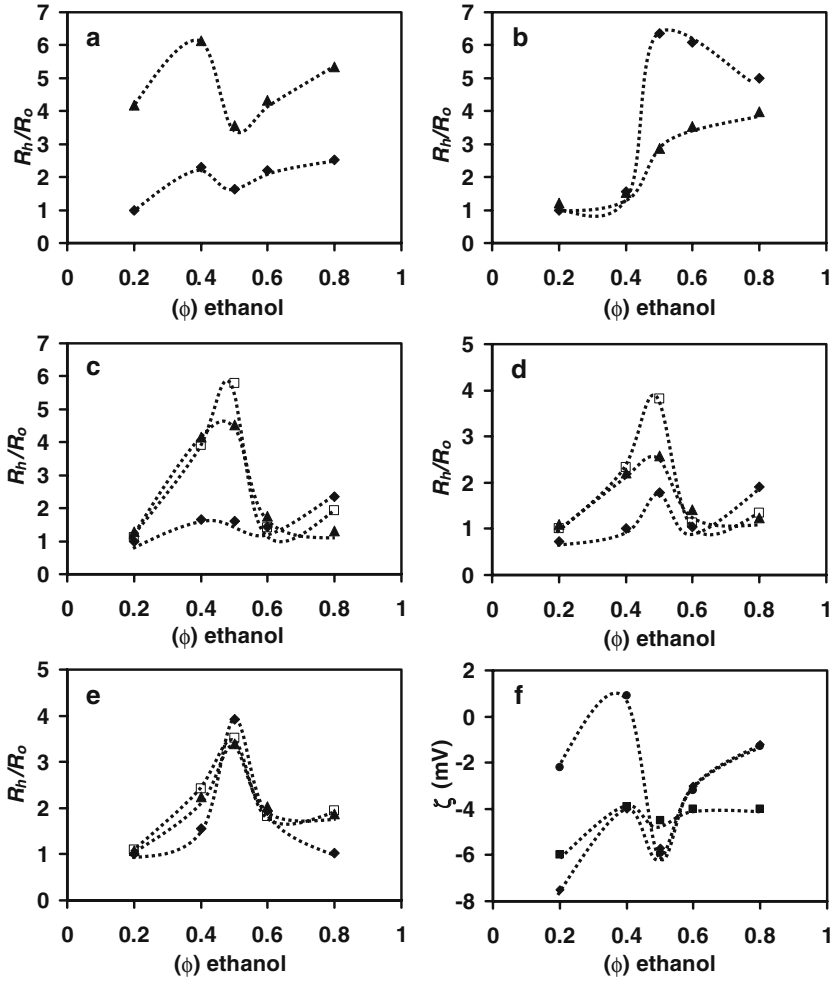

Fig. 6 Variation in R_h/R_0 of microgels in mixed solvents. **a** poly(NIPAm-AA), R_0= 72.1 nm; **b** poly(NIPAm-VI), R_0=122 nm; **c** PA-0.46, p*I*=5.8, R_0=79 nm; **d** PA-0.9, p*I*=5.6, R_0= 73.8 nm;**e** PA-1.65, p*I*=4.75, R_0=57.2 nm, (♦) pH=4.0, (□) pH=pI, (▲) pH=7.5; f Variation in ζ-potential of PA microgels in mixed solvents at the isoelectric point (determined in aqueous solutions): (♦) PA-0.46, (□) PA-0.9, (●) PA-1.65

imidazole groups were protonated), the maximum extent of swelling was relatively small (R_h/R_0≈1.5) while at pH=p*I* (aq)*=5.8 and at pH=7.0, the values of R_h/R_0 were significantly larger (ca 6.0 and 4.5, respectively). For asymmetric PA-1.65 microgels (enriched with AA), the maximum extent of swelling was expected to occur at pH=7.5, similar to poly(NIPAm-AA) microgels; instead, Fig. 6e shows that the extents of swelling at all pH values were in close proximity to each other ($3.5<R_h/R_0<4.0$). For the symmetric PA-0.9 microgel (Fig. 5d), the value of R_h/R_0 at pH=4.0 was ca 1.8 (greater than that for PA-0.46 but smaller than that of PA-1.65). Overall, the extent of swelling of the PA microgels in mixed solvents at pH=4.0 and ϕ≈0.5 correlated with the amount of AA present in the system: an increase in AA content led to greater swelling. However, this effect could not be attributed to coulombic interactions alone because AA groups were not completely ionized at pH=4.0. A possible explanation for this may lie in the nonuniform distribution of functional groups throughout the microgel.

At the values of pH close to p*I*, all PA microgels showed significant swelling at ϕ≈0.5 (molar fraction of ethanol is 0.24). This phenomenon was unexpected because at p*I*, the microgels were believed to be in their most compact state due to electrostatic attraction between the oppositely charged groups. As the isoelectric point for the mixed solvent medium could differ from that in water, we examined the effect of addition of ethanol on ionization of VI and AA groups by measuring ζ-potential of the PA microgels at p*I* (aq) as a function of ϕ (Fig. 6d). The small increase observed at ϕ=0.5 (−4 to −7 mV) (Fig. 6f) was not sufficient to explain the magnitude of the observed changes in size of the PA microgels.

Discussion

The variation in degree of swelling for PE microgels was consistent with the state and nature of the ionic groups in binary copolymers [35, 45, 46]. For example, at pH<4.3 (below pk_a of AA) the anionic poly(NIPAm-AA) microgels remained in a shrunken state while at pH>4.3, they swelled due to repulsion between the deprotonated carboxylic acid groups and their increased hydrophilicity [47]. Similarly, the cationic poly(NIPAm-VI) microgels were in a shrunken state at pH>7.0 (above pk_a of VI) whilst at pH<7.0, protonation of the imidazole groups and subsequent repulsion between them resulted in microgel swelling. The swelling of PA microgels upon change in pH appeared as a *seeming* combination of responses of PE microgels. Outside the zwitterionic window, PA microgels carried a substantial number of similarly charged groups; repulsion between the like charges caused swelling at high and low pH values, similar to PE microgels. Contrastingly, in the zwitterionic window, the PA microgels shrank due to ion pairing between AA and VI residues. The discussion focuses on the volume changes of PA microgels in the zwitterionic region with emphasis on the effects of microgel composition and ion pairing. We stress that in this regime, ion coupling between the oppositely charged groups did not rule out the existence of charged groups excluded from ion pairing.

It is worthwhile to note that the dramatic changes in size we observed for the different microgels were partly due to the low cross-linking density of the microgels. While the distribution of functional groups throughout the microgels is also important and has some bearing both on swelling extent and value of p*I*, the low cross-linking density in the microgels allows for large swelling capacity.

Effect of pH and ionic strength In the zwitterionic window (4.3<p*I*<7.0), the PA microgels shrank due to substantial ion coupling between COO^- and $=NH^+$ groups (Fig. 3a–d). The fractions of positively and negatively charged groups in the microgels played an important role in swelling behavior. The swelling profiles of the microgels with a large fraction of AA or VI fragments had asymmetric shapes with greater swelling at either high or low pH regions, respectively: any contraction that may have occurred due to limited ion pairing was concealed by repulsion between the excess number of like charges in these regions. The swelling profiles of these "asymmetric" PA microgels were similar to those of PE microgels. PA microgels with almost equal amounts of AA and VI showed more symmetric swelling profiles with relatively similar degrees of swelling in regions on both sides of the p*I*. We note that to obtain a "symmetric" volume response, the molar ratios of AA and VI monomers in the batch reaction were carefully tuned, as the reactivity of VI with respect to NIPAm is much greater than that of AA.

Increase in ionic strength caused shrinkage of the PE microgels due to the screening of electrostatic repulsion between like charges. In contrast, PA microgels showed antipolyelectrolyte behavior: the addition of salt weakened the electrostatic intra- and interchain attractions between oppositely charged ionic groups, causing microgel swelling. Contrary to expectations, there was no discernable correlation between the number of ion pairs in the PA microgels and their swelling ratio. Instead, increasing AA content dominated the swelling ratio of PA microgels. This result was in agreement with previous reports on the enhanced swelling of NIPAm-AA microgels with increasing AA content in electrolyte solutions; the hydrophilicity of the AA residues facilitated conformational rearrangement of the polymer chains and in turn, enhanced the degree of microgel swelling [47]. At significantly higher ionic strengths, microgel swelling occurred due to suppressed electrostatic stabilization.

Effect of temperature For both PE and PA microgels in their ionized state, the increase in the onset temperature of the microgel shrinkage in comparison with polyNIPAm

homopolymers (VPTT=31 °C) was due to the presence of the hydrophilic AA and VI segments. The loss in colloidal stability of PA microgels at higher temperatures was ascribed to hydrophobic interactions between the particles, consistent with the behavior of PA microgels reported by Ogawa et al. [29].

The "symmetric" PA microgels exhibited a broader temperature-dependent volume transition and was more stable to deswelling than the "asymmetric" PA microgels, due to the presence of a larger number of hydrophilic COO^- and $\equiv NH^+$ ions in the zwitterionic window (Table 1). However, by contrast with the previous report by Ogawa et al. [29], we observed a greater extent of shrinkage of symmetric PA microgels compared to asymmetric PA microgels. Ogawa et al. [29] reasoned that the larger ion-pair content in the symmetric PA systems acted as "physical cross-links" and that the microgels was already in a highly shrunken state, which limited its deswelling ability upon heating [29]. Admittedly, at p*I*, the PA microgel maintains its smallest size at room temperature (in comparison with its size at other pH values) due to electrostatic attraction between the oppositely charged groups. Nevertheless, in this state, not all charged groups form ion pairs due to the constraints imposed by polymer chain connectivity. We believe that in our work, stronger shrinkage of symmetric PA microgels occurred due to the larger number of ion pairs formed: contraction of the polymer chains brought the charged AA and VI residues closer to each other, enabling previously unpaired charges to couple and enhancing the electrostatic attraction between the already paired groups. Our experiments showed a trend similar to that observed by Lyon et al. [11] who reported that PA microgels underwent greater shrinkage at zwitterionic pH than at non-zwitterionic pH, although the volume phase transitions in our systems were broader [11].

Effect of solvent Introduction of ethanol to aqueous dispersions of PE and PA microgels gave rise to two coexistent phenomena: change in electrostatic interactions and solvency-related effects. For electrostatic effects, two competing factors must be considered. Firstly, the strength of the electrostatic effects in ethanol–water mixtures may increase, as coulombic interactions are stronger in ethanol than in water (the dielectric constants of ethanol and water are 24.3 and 81, respectively). Simultaneously, the net effective charge of the microgels may diminish due to the reduced polarity of the medium and altered pk_a and pk_b values of the ionic groups. The quality of the solvent affects the monomer–monomer and monomer–solvent interactions, the nature of which vary with change in polymer and solvent compositions. Cononsolvency occurs when the mixed medium is a poorer solvent for the particles than either of its pure components, while cosolvency occurs when the mixed medium is a superior solvent for the particles than either of its pure components [45].

Winnik and coworkers have reported the cononsolvency behavior of polyNIPAm in methanol–water mixtures due to the formation of clathrate hydrates [48]. Vincent [49] and Tanaka confirmed that cononsolvency behavior was preserved in poly(NIPAm-AA) microgels containing a small amount of AA or methacrylic acid at $0.4<\phi<0.6$ in ethanol–water mixtures [50]. However, for larger concentrations of AA, poly(NIPAm-AA) microgels showed cosolvency behavior, much like that shown by AA homopolymer gels [51]. In our work, cationic and anionic PE microgels showed different behavior in the range of ethanol concentration $0.4<\phi<0.6$: poly(NIPAm-VI) microgels swelled while poly(NIPAm-AA) microgels shrank. For both PE microgels, the greatest extent of swelling occurred at pH corresponding to their charged states: at pH=7.5 for poly(NIPAm-AA) and at pH=4.0 for poly (NIPAm-VI). Thus, for poly(NIPAm-VI) electrostatic repulsion between the charged $\equiv NH^+$ groups enhanced swelling, while for poly(NIPAm-AA) microgels, repulsion between the $-COO^-$ groups counteracted the deswelling of the system. The pH dependence of the variation in R_h/R_0 indicated the importance of electrostatic effects in microgel swelling, in addition to that of solvent quality.

The swelling properties of PA microgels also originated from the aforementioned solvency and electrostatic effects. The former involved competing solvency (governed by charged AA and VI residues) and cononsolvency (governed by NIPAm residues) effects [31]. The latter could enhance contraction of the PA microgels in the zwitterionic regime due to stronger electrostatic attraction between the oppositely charged groups. Such behavior was observed by Tanaka for bulk PA gels exposed to mixtures of water and ethanol [31].

In our work, all PA microgels showed a swelling maximum at $\phi=0.5$, irrespective of microgel composition or pH value, indicating the overriding influence of solvent quality on microgel swelling. In particular, the notably strong swelling of all PA microgels at pH≈p*I* was unexpected: as the microgels were in their most compact state in the zwitterionic regime, they were expected to resist swelling in this region. The small deviation of electrokinetic potential from zero at $\phi=0.5$ and pH≈p*I* (Fig. 6f) was insufficient to explain the magnitude of the observed changes in R_h/R_0 on the basis of electrostatic interactions.

As at $\phi=0.5$, poly(NIPAm-VI) microgels showed a swelling *maximum*, the swelling of PA microgels at $\phi=0.5$ may have been governed by imidazole–solvent interactions. This justification could also explain the decrease in the value of R_h/R_0 from ca 6 for PA-0.46 (Fig. 6c) to ca 3.5 for PA-1.65 (Fig. 6e) with decreasing VI content in the PA microgels. However, the pH- and composition-dependent variation in R_h/R_0 for the PA microgels indicated that this was not entirely the case: the values of R_h/R_0 for poly (NIPAm-AA) (Fig. 6a) and poly(NIPAm-VI) (Fig. 6b) at pH=7.5 and $\phi=0.5$ were ca 3.5 and 2.7, respectively, implying that, the swelling of all PA microgels at pH=7.5

was driven by *both* AA–solvent and VI–solvent interactions. Furthermore, we recall that for PE microgels at ϕ=0.5, repulsion between the $\equiv NH^+$ groups favored swelling at pH=4.0. However, at ϕ=0.5, R_h/R_0 for PA-0.46 (microgels with highest content of VI) was *lower* at pH=4.0 than at pH=7.5. In fact, at pH=4.0 and ϕ=0.5, *decreasing* content of VI led to a progressive *increase* in the degree of swelling. Even more surprising was the fact that this increased degree of swelling occurred along with the increase in AA content. The latter behavior was also unexpected because the contribution of AA to swelling at pH=4.0 was significantly smaller than that of VI (as determined from the pH-dependent variation in swelling of PE microgels, Fig. 6a,b).

Conclusion

We examined the swelling behavior of polyelectrolyte and polyampholyte microgels in response to the variation in pH, ionic strength, temperature, and solvent composition. Polyampholyte microgels with an excess of either a cationic or an anionic group showed pH-dependent swelling behavior much like that of their polyelectrolyte counterparts. Polyampholyte microgels with symmetric compositions exhibited swelling at both low and high pH ranges. To obtain symmetric swelling in PA microgels at low and high values of pH, the composition of the reaction mixture was tuned to account for the different reactivities of comonomers. In KCl solutions, PA microgels showed antipolyelectrolyte behavior: they swelled with increasing electrolyte concentration. The temperature-dependent volume phase transitions of both PE and PA microgels shifted to higher values than that of polyNIPAm due to the hydrophilicity of ionized AA and VI groups. Ion pairing between charged AA and VI groups increased the extent of the temperature-induced deswelling in PA microgels with symmetric composition. The solvent-dependent swelling behavior of PE and PA microgels showed that competing electrostatic and solvency interactions determined their swelling response. The role of electrostatic effects in PE microgels in ethanol–water mixtures was evident from their increased swelling at pH values corresponding to the ionic states of AA and VI groups. The solvency effects, however, dominated the swelling behavior of all PA microgels, which showed a swelling maximum at ϕ=0.5, irrespective of microgel composition or pH value.

References

1. Saunders BR, Vincent B (1999) Adv Colloid Interface Sci 80:1
2. Senff H, Richtering W (1999) J Chem Phys 111:1705
3. Jeong B, Gutowska A (2002) Trends Biotech 20:305
4. Ogawa Y, Ogawa, K, Wang B, Kokufuta E (2001) Langmuir 17:2670
5. Lopez V, Castro, Snowden MJ (2003) Drug Delivery Systems and Sciences 3:19
6. Kiser PF, Wilson G, Needham D (1998) Nature 394:459
7. Nayak S, Lee H, Chmielewski J, Lyon LA (2004) J Am Chem Soc 126:10258
8. Morris GE, Vincent B, Snowden MJ (1997) Progr Colloid Polym Sci 105:16
9. Retama JR, Lopez-Ruiz B, Lopez-Cabarcos E (2003) Biomaterials 24:2965
10. Xu S, Zhang J, Paquet C, Kumacheva E (2003) Adv Funct Mater 13:468
11. Lyon LA, Kong SB, Eustis S, Debord JD (2002) Polym Prepr 43:24
12. Zhang J, Xu S, Kumacheva E (2004) J Am Chem Soc 26:7908
13. Xu S, Zhang J, Kumacheva E (2003) Compos Interfaces 10:405
14. Saunders BR (2004) Langmuir 20:3925
15. Stieger M, Pedersen JS, Lindner P, Richtering W (2004) Langmuir 20:7283
16. Pelton R (2004) Macromolecular Symp 207:57
17. Hoare T, Pelton R (2005) Polymer 46:1139
18. Debord JD, Lyon LA (2003) Langmuir 19:7662
19. Jones CD, Lyon LA (2000) Macromolecules 33:8301
20. Nolan CM, Serpe MJ, Lyon LA (2004) Biomacromolecules 5:1940
21. Pinkrah VT, Snowden MJ, Mitchell JC, Seidel J, Chowdhry BZ, Fern GR (2003) Langmuir 19:585
22. English A, Salvador M, Jose A, Manzanares XY, Grosberg A, Tanaka T (1996) J Chem Phys 104:8713
23. Fernandez-Nieves A, Fernandez-Barbero A, De las Nieves FJ, Vincent B (2000) J Physics Condens Matter 12:3605
24. Neyret S, Vincent B (1997) Polymer 38:6129
25. Tanaka T, Fillmore DJ (1979) J Chem Phys 70:1214
26. Zhous S, Chu B (1998) J Phys Chem B 102:1364
27. Heijl JMD, Du Prez FE (2004) Polymer 45:6771
28. Bromberg L, Temchenko M, Alakhov V, Hatton TA (2005) Langmuir 21:1590
29. Ogawa K, Nakayama A, Kokufuta E (2003) Langmuir 19:3178
30. Nayak SP, Lyon LA (2003) Polymer Prepr 44:679
31. Tanaka T (1978) Phys Rev Lett 40:820
32. Bradley M, Ramos J, Vincent B (2005) Langmuir 21:1209
33. Takeoka Y, Berker AN, Du R, Enoki T, Grosberg A, Kardar M, Oya T, Tanaka K, Wang G, Yu X, Tanaka T (1999) Phys Rev Lett 82:4863
34. Madaeni S, Ghanbarian M (2000) Polymer Intl 49:1356
35. Hoare T, Pelton R (2004) Macromolecules 37:2544
36. Datta SP, Grybowski AK (1966) J Chem Soc B 136
37. Kodama H, Miyajima T, Tabuchi H, Ishiguro S (2000) Colloid Polym Sci 278:1–7
38. Molina MJ, Gomez-Anton MR, Pierola IF (2004) J Polym Sci B 42:2294–2307
39. Schilling S, Niestroj AJ, Rahfeld J-U, Hoffmann T, Wermann M, Zunkel K, Wasternack C, Demuth H-U (2003) J Biol Chem 278(50):49773–49779
40. Molina MJ, Gomez-Anton MR, Pierola IF (2002) Macromol Chem Phys 203:2075–2082

41. Crowther HM, Saunders BR, Mears SJ, Cosgrove T, Vincent, B, King SM, Yu GE (1999) Colloid Surf A Physicochem Eng Asp 152:327
42. Bokias G, Staikos G, Iliopoulos I (2000) Polymer 41:7399
43. Tiera MJ, Santos GR, Tiera VA, Vieira NAB, Frolini E, Da Silva RC, Loh W (2005) Colloid Polym Sci 283:662
44. Li Y, Kwak JCT (2004) Langmuir 20:4859
45. Christensen ML, Keiding K (2005) Colloids Surf A Physicochem Eng Aspects 252:61
46. Hoare T, Pelton R (2005) Polymer 46:1139
47. Snowden MJ, Chowdhry BZ, Vincent B, Morris GE (1996) J Chem Soc Faraday Trans 92:5013
48. Winnik F, Ottaviani F, Bossman SH, Garcia-Garibay M, Turro JN (1992) Macromolecules 25:6007
49. Saunders BR, Crowther HM, Vincent B (1997) Macromolecules 30:482
50. Amiya T, Hirokawa Y, Hirose Y, Li Y, Tanaka T (1987) J Chem Phys 86:2375
51. Ikkai F, Masui N, Karino T, Naito S, Kurita K, Shibayama M (2003) Langmuir 19:2568